JACS
JOURNAL OF THE AMERICAN CHEMICAL SOCIETY
pubs.acs.org/JACS
Article

Hydrocarbon Degradation by Contact with Anoxic Water Microdroplets

Xuke Chen,[‖] Yu Xia,[‖] Zhenyuan Zhang,[‖] Lei Hua, Xiuquan Jia,* Feng Wang, and Richard N. Zare*

Cite This: J. Am. Chem. Soc. 2023, 145, 21538−21545

ABSTRACT: Oils are hydrophobic, but their degradation is frequently found to be accelerated in the presence of water microdroplets. The direct chemical consequences of water−oil contact have long been overlooked. We show that aqueous microdroplets in emulsified water−hexadecane ($C_{16}H_{34}$) mixtures can spontaneously produce CO_2, •H, H_2, and short-chain hydrocarbons (mainly C_1 and C_2) as detected by gas chromatography, electron paramagnetic resonance spectroscopy, and mass spectrometry. This reaction results from contact electrification at the water−oil microdroplet interface, in which reactive oxygen species are produced, such as hydrated hydroxyl radicals and hydrogen peroxide. We also find that the H_2 originates from the water microdroplet and not the hydrocarbon it contacts. These observations highlight the potential of interfacial contact electrification to produce new chemistry.

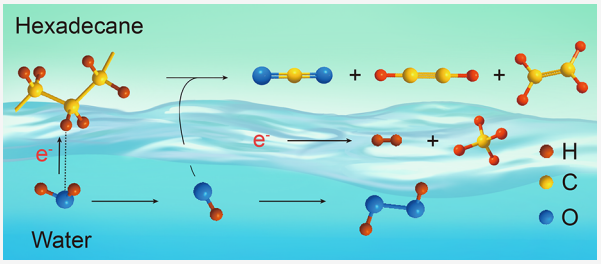

INTRODUCTION

Water is the most abundant substance on the Earth's surface, and it ubiquitously forms charged interfaces caused by preferential adsorption of positive or negative ions at the surface where the hydrophobic and hydrophilic phases meet. As will be shown, this contact electrification can allow us to manipulate chemical transformations that otherwise would not occur in bulk water. Recent work suggests that electron transfer dominates contact electrification between water and a hydrophobic medium.[1] This electron transfer at water microdroplet interfaces is more recently shown to give rise to unexpected redox reactions.[2] The potential applications of this chemistry range from ecosystem to industry, where contact electrification at the water−gas and water−solid interfaces of water microdroplets makes possible formation of aqueous reactive oxygen species (ROS) and what are believed to be hydrogen radical (•H).[3−13] We extend the contact-electric redox chemistry to the highly deformable water−oil microdroplet interfaces by describing the spontaneous generation of H_2 and ROS from microdroplets of water in contact with the model oil hydrocarbon, hexadecane, which leads to the evolution of CO_2 and the production of short-chain hydrocarbons (mainly C_1 and C_2).

Gaseous hydrocarbons in the natural environment, mainly C_1 and C_2, are important energy resources and greenhouse gas. Their formation can be biotic or abiotic in origin. Conventional models predict that abiotic gases created from the thermal cracking of oil form above ∼150 to 160 °C.[14,15] At lower temperatures, methane is considered to be generated dominantly by microbes.[16] In recent years, the origin of methane from abandoned oil wells has been ascribed as predominantly thermogenic, with light hydrocarbon concentration ratios (C_{2-4}/C_1) much higher than microbial sources.[17] However, no positive correlation was observed between the concentration of the emitted methane and the well depth,[18,19] although the thermal cracking of oil in a reservoir into gas is a consequence of the rising temperature that accompanies increasing burial depth.[20] Thus, the question has remained unsettled regarding whether the overlooked abiotic origins of gaseous hydrocarbons exist at low temperatures. Considering the common occurrence of very stable or even permanent aqueous microdroplets in oil wells arising from the coproduction of water and oil,[21] we present evidence that this might be a previously unrecognized source of methane. We suggest that water−oil microdroplet chemistry may be important for interpreting and manipulating oil transformations.

In this regard, it is well-known that adding water to diesel oil to form a fuel emulsion is advantageous in providing diesel engines more power and less pollution from unburnt hydrocarbons and NO_x.[22,23] A number of reasons have been advanced to explain this fact:[24,25] the reduction of the maximum temperature of the combustion chamber that can reduce NO_x formation owing to the large latent heat for water evaporation, the accelerated oxidation of soot by reaction with water, and microexplosions of evaporating water droplets that

Received: July 12, 2023
Published: September 19, 2023

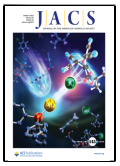

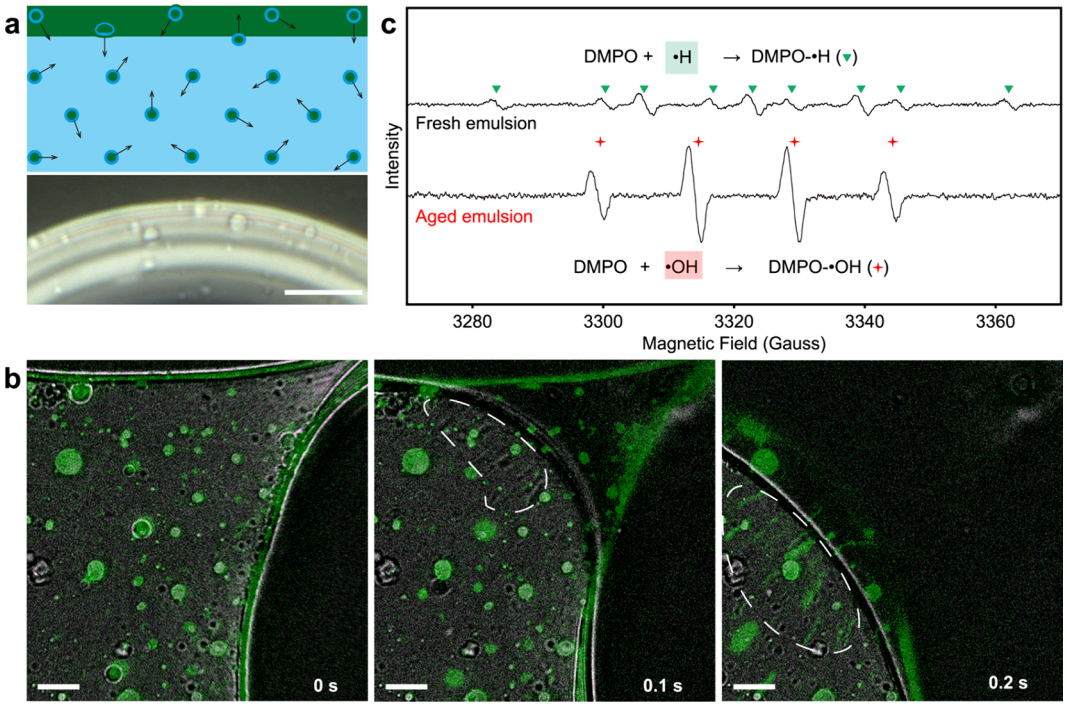

Figure 1. Water−hexadecane emulsion. (a) Schematic illustration and microscopy of the water−oil microdroplets. Here, green represents oil, light blue represents bulk water, and dark blue represents hydrophobic hydration shell. (b) Brightfield/fluorescence merged images of dynamic water−hexadecane contact. (c) Observed formation of •H and •OH in the emulsion and anaerobically aged emulsion in Ar with EPR spectroscopies. Scale bars: 10 μm (a, b). Dashed circles indicate the zone for the refilling of cavities.

can increase fuel-air mixing and reduce soot formation. We hypothesize that the ability of water microdroplets to transform long-chain hydrocarbons to short-chain hydrocarbons and to produce H_2 might be another important contributing factor.

Here, with hexadecane as the oil model, we report the spontaneous generation of a redox reaction at the water−oil interface of the aqueous microdroplets in emulsion as a result of a mechanism based on contact-electric charging, followed by the reduction of water that leads to the evolution of H_2 and the formation of ROS, such as the hydroxyl radical (•OH) and hydrogen peroxide (H_2O_2). The spontaneous cracking on both the hydrophobic and aqueous sides of the droplet interface shows that water−oil contact can cause considerable chemical consequences at normal temperatures.

RESULTS AND DISCUSSION

Highly Deformable Water−Oil Microdroplet Interfaces. In an enclosed system, deoxygenated ultrapure water was mixed with hexadecane and nebulized using high-frequency (2.4 MHz) ultrasonication, which exhibits low dissociation of water,[26] for 4 h, as shown in Figure S1, resulting in a water−hexadecane emulsion. The small size of microdroplets in this ultrasound-prepared emulsion, consisting of microdroplets with an average diameter of 5.4 μm and submicrometer droplets with an average diameter of 0.25 μm, resulted in a stable emulsification that lasted for more than a week (Figures S2 and S3). The emulsion was thoroughly purged 15 times using argon gas (inflated to 2 atm and then released to atmospheric pressure) and subjected to a vacuum treatment for 20 min (10 min for H_2) to eliminate potential H_2 and C_1−C_2 products formed during the ultrasonication process. Then, the aforementioned purging process was repeated to further mitigate possible interference of the ultrasonication process on subsequent experimental results. It is well-known that ultrasonication of water can produce radicals.[27,28] In order to demonstrate that the H_2 generated from the evacuated emulsion is not a result of dissolution during ultrasonication followed by slow release from the emulsion, we used a simple titration method that employs a methylene blue-platinum colloid reagent to determine the concentration of H_2 in an aqueous solution.[29] One drop of the colloid reagent reacts with approximately 100 ppb of H_2 dissolved in 6 mL of water, equivalent to 0.3 μmol of H_2. If more than 0.3 μmol of H_2 dissolves in the solution, the color will change from blue to colorless. We added 1 mL of water solution containing a drop of the reagent to each of the two different samples: a H_2 saturated water solution and a fresh emulsion after ultrasonication and evacuation. We found that the H_2-saturated water solution remained colorless throughout the injection of the reagent solution (Movie S1), while the evacuated emulsion quickly turned blue without color fading (Movie S2). This indicates that H_2 dissolved in the emulsion is less than 0.3 μmol. Thus, the H_2 of more than 0.3 μmol that is produced from the evacuated emulsion cannot come from the residual H_2 in the fresh emulsion. We are confident that the experiments we describe next are free from artifacts caused by the preparation of the oil−water emulsion. The resulting oil−water emulsion is then sprayed by nebulization using argon gas.

A violent fluctuation in the position of these aqueous droplets was observed (Figure 1a and Movie S3) in the emulsion, which may be described as a Brownian motion. To obtain insight into the deformable water−oil interface, we analyzed the breakup behavior of the stretched emulsion on a glass slide using Nile red fluorescence microscopy (Figure 1b).

https://doi.org/10.1021/jacs.3c07445
J. Am. Chem. Soc. 2023, 145, 21538−21545

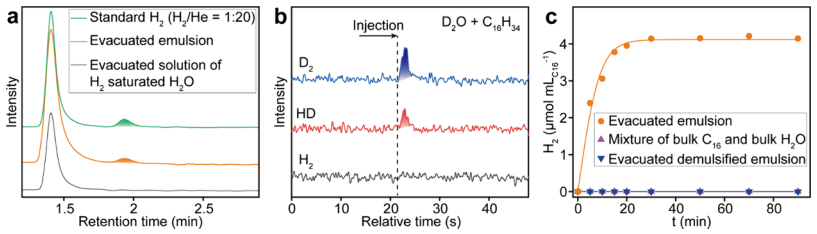

Figure 2. Evolution of H_2. (a) GC spectra of H_2 escaping from evacuated aqueous solution in 90 min using 2 mL of He as internal standard. (b) Mass spectrometric detection of hydrogen gas in the gas phase above evacuated D_2O-hexadecane emulsion. (c) Time course of H_2 product formation.

The alkane-sensitive fluorescent probe of Nile red demonstrated a hexadecane coating at the surface of the emulsion droplet as well as the existence of submicrometer-sized aqueous hexadecane droplets in the emulsion. A fast contraction of water was observed after the ligament breakup (Movie S4). It was found that hexadecane did not tend to drift along the contracting water. This led to the separation of the hexadecane-coated layer from the emulsion surface within 0.1 s of ligament breakup. In the subsequent 0.2 s, the residual oil layer flowed to the exposed water surface as a result of the Marangoni effect (Figure S5). In the emulsion, the formation of stretched cavities stripped of hexadecane was observed in the initial 0.1 s, and these cavities were refilled with hexadecane in the following 0.2 s. We can deduce that Brownian motion of submicro- and microdroplets would enable similar destruction and restoration of the water−oil contact between the hexadecane droplets and hydrophobic hydration shells.

Although no solvated electrons have been directly observed at this time, we believe that this dynamic behavior of deformable water−oil interface, which exhibits charge transfer across C−H···O hydrogen bonds at the water−oil interface,[30] satisfies the conditions for contact-electric charging that can be facilitated during the approach-contact-separation process.[31] This was verified by the indirect observation of •OH and •H in the emulsion with electron paramagnetic resonance (EPR) spectroscopies using 5,5-dimethyl-1-pyrroline *N*-oxide (DMPO) as the probe (Figure 1c). As shown in the publication by Chen et al.[2] and supported by many studies of Wang and co-workers,[1,32,33] the electron transfer comes about through contact electrification and the development of a strong electric field at the interface. It is also facilitated by the loss of three-dimensional hydrogen bonding through the development of partial solvation of the two ions. As we have shown in the formation of H_2O_2 by the condensation of water vapor, friction is unnecessary to cause contact electrification.[34] Simple contact is sufficient. •H disappeared upon subsequent aging of the emulsion under stirring in an argon (Ar) atmosphere for 1.5 h. The hydroxyl radical •OH represents the primary radical in the aged emulsion. These results imply the spontaneous switching of redox properties from reductive to oxidative in the emulsion, possibly owing to the evolution of reduction products that can carry electrons away from the emulsion.

Evolution of H_2 from the Water−Hexadecane Emulsion. The existence of electrons that come about accompanying the formation of •OH at the gas−water interface of the microdroplets has been supported by the unique reduction reaction over water microdroplets.[3,5,6,35−39] Formation of H_2 has been suggested to be the fate of the electrons pulled from the water microdroplet interface.[40,41] To verify the possible formation of H_2 at the water−oil microdroplet interface, we initially evacuate the fresh emulsion for 10 min, which can exclude interference from potentially dissolved H_2 in water (Figure 2a, see the materials for the detailed procedure). The absence of dissolved H_2 in the fresh evacuated emulsion was further confirmed by the molecular hydrogen test kit that can detect dissolved H_2 at ppb level[29] (Movies S1 and S2). Then, the evacuated emulsion was sealed, charged with Ar, and aged for 1.5 h while stirring. We observed the generation of H_2 in the atmosphere above the aged water−hexadecane emulsion with both gas chromatography (GC) (Figure 2a) and mass spectrometry (MS) (Figure 2b, Figure S6). D_2 and DH instead of H_2 was observed upon replacing H_2O with D_2O (Figure 2b), confirming that H_2 primarily comes from water and not the hydrocarbon. Figure 2c shows the time course of H_2 evolution measured using GC (See the materials, Figure S7 for the GC spectrum). In contrast to the emulsion, the bulk mixture of hexadecane and water did not produce H_2. Moreover, demulsification with dioxane completely extinguished the H_2 evolution. Thus, the water−oil interface of a microdroplet has been unambiguously demonstrated to be capable of producing H_2. Herein, H_2 evolution could also be observed over the evacuated emulsion in the absence of stirring (Figure S8), verifying that simple contact is sufficient for electron transfer at the interface. The H_2 evolution reaction proceeded but reached a plateau after 0.5 h. It was found that about 4 μmol of H_2 was generated per milliliter of $C_{16}H_{34}$ (see the materials, Figure S9 for the standard curve), indicating a gradual detachment of electron from the microdroplets in emulsion, which should be accompanied by generation of ROS and organic oxidation reactions. The subsequent generation of H_2 might be hindered by the accumulation of aqueous ROS and other oxidative products as competitive electron acceptors or H_2 scavengers at water interfaces.

ROS Formation and Subsequent Oxidation Reactions at the Water−Oil Microdroplet Interface. To investigate the possible ROS formation reactions that may emerge at the water−oil interface of microdroplets, we performed fluorescent microscopy with the H_2O_2-sensitive water-soluble probe, 10-acetyl-3,7-dihydroxyphenoxazine, for hexadecane-dispersed water droplets prepared in a microfluidic chip. Water microdroplets spontaneously generate ROS during contact with hexadecane, as evidenced by the gradual appearance of orange fluorescence (Figure 3a, Movie S5). The accumulation of ROS over the water−oil interface of the water microdroplet is slow but long-lasting relative to the water−silica system, which reached a maximum value within seconds.[2] This sustained increase in ROS concentration might result from the continuous evolution of H_2 and other electron carriers.

The transformation of interfacial oil might also be noteworthy if inert water could be split at the water−oil

https://doi.org/10.1021/jacs.3c07445
J. Am. Chem. Soc. 2023, 145, 21538−21545

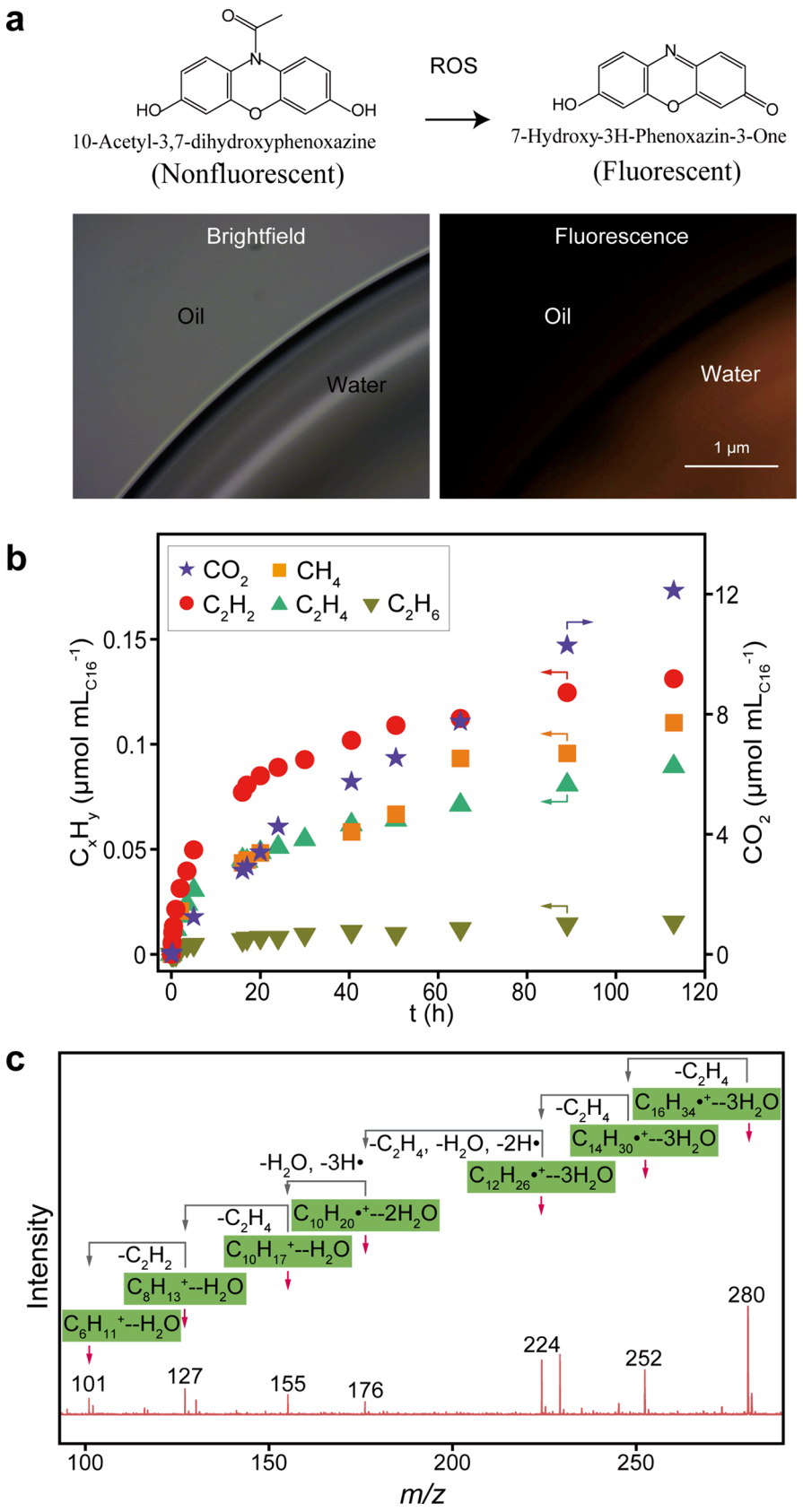

Figure 3. ROS and C_1−C_2 gaseous product formation. (a) Fluorescence microscopy images of ROS generation in a hexadecane-dispersed water droplet. (b) Time course of C_1−C_2 products from the evacuated emulsion. (c) Observed formation of alkane radical cations determined by mass spectrometry.

https://doi.org/10.1021/jacs.3c07445
J. Am. Chem. Soc. 2023, 145, 21538−21545

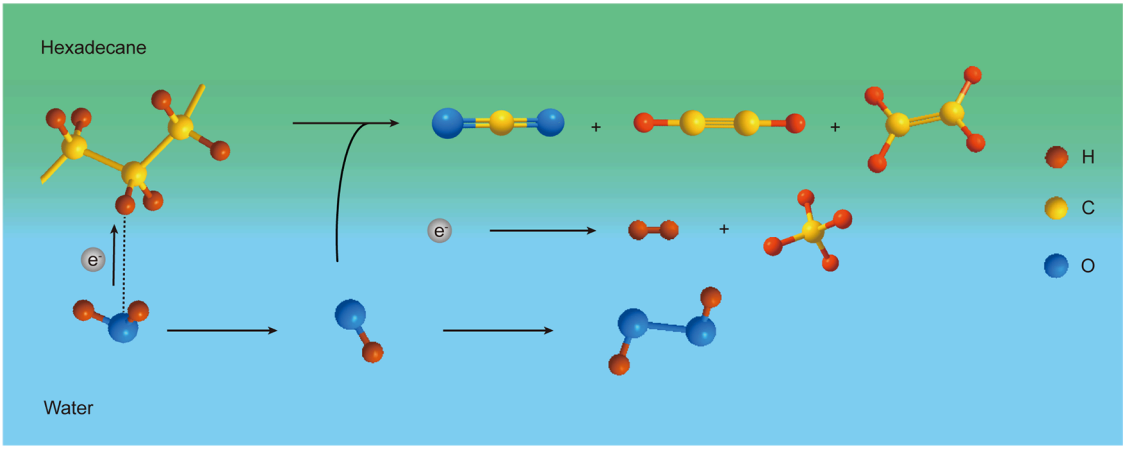

Figure 4. Schematic overview of the contact-electric chemical reactions at the water/oil microdroplet interfaces.

interface of microdroplets. After evacuating the fresh emulsion (see the materials for the detailed procedure), CO_2 was observed as the primary gaseous product (Figure 3b), possibly produced by the complete oxidation reaction with aqueous •OH. Accompanied by CO_2 evolution, C_1-C_2 hydrocarbons, mainly C_2H_2, were detected in the gas phase (Figure 3b; see the materials, Figures S10−S12 for the GC spectra, Figure S13 for the MS spectrum of C_2H_2), demonstrating the power of the water microdroplet interface to crack hydrocarbons. Although the proportion of methane increased upon prolonging the aging time, its fraction remained lower than that of C_2 hydrocarbons in 120 h. The low fraction of methane might result from the inefficient hydrogenation of CO_2. This is quite different from the conventional anaerobic oil degradation by microorganisms, in which formation of CH_4 is predominant.[16,42] Carbon monoxide (CO) is an important product in aqueous reforming reactions driven by solar and ultrasonic energy. Herein, no CO was observed (Figure S14), indicating that the cracking reaction pathway at the water−oil interface of microdroplets in emulsion is distinctive.

To understand how hexadecane was cracked into C_2 hydrocarbons, the intermediate species in the emulsion were probed using MS without applied potential (Figure 3c, Figures S15−S17). To minimize the possible iron contamination that might lead to Fenton reactions at the water interface,[43,44] silica tubing instead of stainless-steel tubing was used to export the emulsion to the MS inlet. The cationic adducts of hexadecane, *n*-tetradecane, and *n*-dodecane with three H_2O were observed at *m*/*z* 280, 252, and 224, respectively, indicating the occurrence of sequential C−C bond fragmentation which yields C_2 fragments. As the ionization potential of water (12.58 eV for water trimer)[45] is much higher than the ionization potential of hexadecane (9.64 eV),[46] the possibility of a neutral alkane molecule combined with a $H_2O•^+(H_2O)_2$ cation could be ruled out. The C−C bond fragmentation by losing C_2 intermediates is a typical process for long-chain alkane σ radical cations,[47,48] which is consistent with the formation of C_2 hydrocarbons (Figure 3c). Therefore, we conclude that the microdroplet generated the $C_nH_{2n+2}•^+$ adduct of three H_2O. Apart from the $C_nH_{2n+2}•^+$--$3H_2O$ cations, a strong peak with an *m*/*z* of 229 was detected, which is ascribed to mono-(2-hydroxyethyl) terephthalic acid--H_3O^+ (MHET--H_3O^+) leached from the PET container. This is consistent with a previous report showing that $H_3O^+(H_2O)_2$ became the dominant water cluster ions under the circumstance of room temperature and extremely low water vapor pressure in the MS.[49] According to the presence of hydrates of alkane σ-radical cations, the microdroplet •OH and •H are proposed to be consumed in the oxidative cracking of hexadecane, which might explain the above-mentioned slow accumulation of ROS. Subsequent C−C bond fragmentation to the products in the 100−176 Da region also yields C_2 fragments. Additional loss of •H or H_2 was observed over the products with lower carbon numbers.

Mechanism of the Contact-Electric Chemical Reactions at the Water−Oil Microdroplet Interface. An outline for the aqueous oil autoxidation reaction driven by contact electrification at the water−oil microdroplet interface can be developed based on the above results (Figure 4). The evolution of H_2 from •H led to electron detachment from the water−oil microdroplet interface. Concomitantly, ROS consisting of •OH and H_2O_2 were spontaneously formed and accumulated as a result of electron detachment. Microdroplet ROS could oxidatively crack the hexadecane to C_2 hydrocarbons via generating cationic radical intermediates of $C_nH_{2n+2}•^+$--$3H_2O$, as well as completely oxidize hexadecane to CO_2. The e^-_{aq} as well as •H could reduce the cracked products to afford saturated short-chain alkanes, such as methane and ethane. Since the initial evolution of H_2 led to the electron detachment from the water−oil microdroplet interface and the accumulation of aqueous ROS in emulsion, the oxidation reaction predominated the cracking of hydrocarbons at the water−oil microdroplet interfaces of emulsion. This might account for the higher abundance of C_2H_2 as the oxidative product in comparison with C_2H_6 as the reductive product.

More mechanistic interpretations are required to elucidate what happens at the oil−water interface. Given the electric field created by the contact electrification, we consider a possible reaction pathway initiated by the enhanced autoionization of interfacial water dimer $[(H_2O)_2]_i$, which has been called the Wien effect:[50]

$$[(H_2O)_2]_i \rightarrow H_3O^+ + OH^- \quad (1)$$

The OH^- and H_3O^+ cluster together at the interface, with a preference for one or the other to be at the extreme outside. This charge separation provides a strong localized electric field that can drive processes that cannot otherwise occur in the bulk water. Herein, this electric field drives the loss of electrons from OH^-[51] to form •OH and from $(H_2O)_2$[52] to form •OH-

https://doi.org/10.1021/jacs.3c07445
J. Am. Chem. Soc. 2023, 145, 21538−21545

H_3O^+. This gives rise to a measurable current for a solid interface, which we have observed.[2] This may also account for the electrons being formed. The electrons can be accepted by H^+ ions to form •H. We also have the process occurring at the interface $H^+ + OH^- \rightarrow$ •H + •OH, as proposed by Colussi.[39] Hence, at the interface but not the bulk or the interior of the droplet, we have

$$OH^- + H_3O^+ \rightarrow \bullet OH + \bullet H + H_2O \quad (2)$$

This reaction is aided by the partial desolvation of H^+ and OH^- at the interface.[10] The H atom can go on to hydrogenate other species at the interface such as N_2 adsorbed on a metal oxide surface,[53] but it can also recombine with itself, •H + •H $\rightarrow H_2$.

The H atom is more likely to react with water because of the overwhelming presence of water:

$$\bullet H + H_2O \rightarrow H_2 + \bullet OH \quad (3)$$

The •H may also react with hydrocarbon RH to form H_2 + R•.[54] The R• might go on to fragment or form a double bond.

The hydroxyl radicals do recombine to form hydrogen peroxide:

$$\bullet OH + \bullet OH \rightarrow HOOH \quad (4)$$

By adding together eqs 1−4, we have the overall reaction:

$$[(H_2O)_2]_i \rightarrow HOOH + H_2 \quad (5)$$

Support for this mechanism is provided by the observation of •H by electron paramagnetic resonance spectroscopy (Figure 1c) and H_2 by gas chromatography (Figure 2a) and mass spectrometry (Figure 2b).

It should be noted that the liquid−liquid interface is not identical with the gas/solid−liquid interface. The distance of electron transfer from the aqueous side to the oil side of the water−oil interface has been investigated by Poli et al.[55] and Pullanchery et al.[30] In the electron-stripped aqueous side of the water−oil interface, there is a layer >1 nm, which has charge density oscillations. In comparison, the water−gas interface is only ∼2 solvation layers deep, having a thickness within 0.35 nm.[56] In addition, the ejected electrons are quite delocalized over all interfacial oil molecules and can penetrate up to ∼0.5 nm into the oil phase. Pullanchery et al. demonstrated that water at the oil droplet surface had a stronger H-bonding network compared with the planar air−water interface,[30] which might account for the longer thickness of water−oil interfaces. Based on these pioneering works, we tentatively propose that the relatively long thickness of the water−oil interface leads to increased charge separation distance, which should be beneficial to the spontaneous formation and stabilization of H_2 and reactive oxygen species.

Implications for Engineering Water−Oil Contact-Electric Microdroplet Chemistry. The present experimental observations clearly suggest that the contact-electric chemistry of the water−oil microdroplet interface in emulsion offers a guide to addressing contemporary environmental and energy challenges. For example, in order to satisfy the requirement of aircraft and ship engines for cleaner fuels,[57−59] researchers have been motivated to conduct research on water-fuel emulsions that can reduce nitrogen oxides and smoke emissions.[23,60] We suggest a previously unrecognized mechanism that is important to engineering the emulsion fuel, namely, the action of water droplets in transforming long-chain hydrocarbons to short-chain hydrocarbons, as demonstrated in the studies made by us. In addition, contact chemistry might be of potential importance for the petroleum industry, considering the existence of large amounts of water as well as oil hydrocarbons in reservoirs after normal oil extraction. Nonmicrobial methane that is not in economically substantial amounts forms in abandoned reservoirs over multiple years and likely decades,[18] which contributes to greenhouse gas levels that adversely affect the environment.[19] If the gasification of remaining oil hydrocarbons can be accelerated by emulsification with water and rational contact-electrocatalyst design, the profitable recovery of fossil fuels, particularly as value-added C_2 hydrocarbons, might be greatly enhanced.

In summary, we have shown that contact electrification at water−oil microdroplet interfaces in an emulsion initially enabled a spontaneous evolution of H_2 and the accumulation of ROS. The accumulation of ROS in the aqueous microdroplets leads to the oxidative cracking of oil at ambient temperature to produce CO_2, CH_4, C_2H_6, C_2H_4, and C_2H_2. Hence, the demonstration of the unique features of contact-electric microdroplet chemistry in aqueous hydrocarbon degradation may fundamentally change our view of oil degradation in reservoirs and how oil−water emulsions confer benefits in combustion engines. The present study also demonstrates the power of oil−water contract electrification in affecting chemical transformations.

■ ASSOCIATED CONTENT

Supporting Information

The Supporting Information is available free of charge at https://pubs.acs.org/doi/10.1021/jacs.3c07445.

Experimental methods, photographs of experimental setup and emulsion, size distribution of droplets in emulsion, mass spectrometric detection of H_2 and C_2H_2, GC spectra, schematic of the home-built TOF-MS, and mass spectrum supporting the data in the main text (PDF)

H_2-saturated water solution remaining colorless throughout the injection of the reagent solution (MP4)

Evacuated emulsion quickly turning blue without color fading (MP4)

Violent fluctuation in the position of aqueous droplets (MP4)

Fast contraction of water after the ligament breakup (MP4)

Water microdroplets spontaneously generating ROS during contact with hexadecane (MP4)

■ AUTHOR INFORMATION

Corresponding Authors

Xiuquan Jia − *State Key Laboratory of Catalysis, Dalian Institute of Chemical Physics, Chinese Academy of Sciences, Dalian 116023, P. R. China;* orcid.org/0000-0002-9921-234X; Email: jiaxiuquan@dicp.ac.cn

Richard N. Zare − *Department of Chemistry, Stanford University, Stanford, California 94305, United States;* orcid.org/0000-0001-5266-4253; Email: zare@stanford.edu

Authors

Xuke Chen − *State Key Laboratory of Catalysis, Dalian Institute of Chemical Physics, Chinese Academy of Sciences,*

Dalian 116023, P. R. China; University of Chinese Academy of Sciences, Beijing 100049, P. R. China

Yu Xia − *Department of Chemistry, Stanford University, Stanford, California 94305, United States;* orcid.org/0000-0001-7647-4921

Zhenyuan Zhang − *State Key Laboratory of Catalysis, Dalian Institute of Chemical Physics, Chinese Academy of Sciences, Dalian 116023, P. R. China; University of Chinese Academy of Sciences, Beijing 100049, P. R. China*

Lei Hua − *State Key Laboratory of Catalysis, Dalian Institute of Chemical Physics, Chinese Academy of Sciences, Dalian 116023, P. R. China*

Feng Wang − *State Key Laboratory of Catalysis, Dalian Institute of Chemical Physics, Chinese Academy of Sciences, Dalian 116023, P. R. China;* orcid.org/0000-0002-9167-8743

Complete contact information is available at: https://pubs.acs.org/10.1021/jacs.3c07445

Author Contributions

‖X.C., Y.X., and Z.Z. contributed equally.

Notes

The authors declare no competing financial interest.

■ ACKNOWLEDGMENTS

This work was supported by the National Key R&D Program of China (2022YFA1504603) and the National Natural Science Foundation of China (22025206, 22172163, 21991094). R.N.Z. and Y.X. also acknowledge support from the US Air Force Office of Scientific Research through the Multidisciplinary University Research Initiative program (AFOSR FA9550-21-1-0170).

■ REFERENCES

(1) Lin, S.; Xu, L.; Chi Wang, A.; Wang, Z. L. Quantifying electron-transfer in liquid-solid contact electrification and the formation of electric double-layer. *Nat. Commun.* **2020**, *11* (1), 399.

(2) Chen, B.; Xia, Y.; He, R.; Sang, H.; Zhang, W.; Li, J.; Chen, L.; Wang, P.; Guo, S.; Yin, Y.; Hu, L.; Song, M.; Liang, Y.; Wang, Y.; Jiang, G.; Zare, R. N. Water-solid contact electrification causes hydrogen peroxide production from hydroxyl radical recombination in sprayed microdroplets. *Proc. Natl. Acad. Sci. U.S.A.* **2022**, *119* (32), No. e2209056119.

(3) Lee, J. K.; Samanta, D.; Nam, H. G.; Zare, R. N. Micrometer-sized water droplets induce spontaneous reduction. *J. Am. Chem. Soc.* **2019**, *141* (27), 10585−10589.

(4) Mehrgardi, M. A.; Mofidfar, M.; Zare, R. N. Sprayed water microdroplets are able to generate hydrogen peroxide spontaneously. *J. Am. Chem. Soc.* **2022**, *144* (17), 7606−7609.

(5) Zhao, L.; Song, X.; Gong, C.; Zhang, D.; Wang, R.; Zare, R. N.; Zhang, X. Sprayed water microdroplets containing dissolved pyridine spontaneously generate pyridyl anions. *Proc. Natl. Acad. Sci. U.S.A.* **2022**, *119* (12), No. e2200991119.

(6) Song, X.; Meng, Y.; Zare, R. N. Spraying Water Microdroplets Containing 1,2,3-Triazole Converts Carbon Dioxide into Formic Acid. *J. Am. Chem. Soc.* **2022**, *144* (37), 16744−16748.

(7) Xing, D.; Meng, Y.; Yuan, X.; Jin, S.; Song, X.; Zare, R. N.; Zhang, X. Capture of hydroxyl radicals by hydronium cations in water microdroplets. *Angew. Chem. Int. Ed.* **2022**, *61* (33), No. e202207587.

(8) Meng, Y.; Gnanamani, E.; Zare, R. N. Direct C(sp^3)-N bond formation between toluene and amine in water microdroplets. *J. Am. Chem. Soc.* **2022**, *144* (43), 19709−19713.

(9) Meng, Y.; Gnanamani, E.; Zare, R. N. Catalyst-free decarboxylative amination of carboxylic acids in water microdroplets. *J. Am. Chem. Soc.* **2023**, *145* (1), 32−36.

(10) Heindel, J. P.; Hao, H.; LaCour, R. A.; Head-Gordon, T. Spontaneous formation of hydrogen peroxide in water microdroplets. *J. Phys. Chem. Lett.* **2022**, *13* (43), 10035−10041.

(11) Li, K.; Guo, Y.; Nizkorodov, S. A.; Rudich, Y.; Angelaki, M.; Wang, X.; An, T.; Perrier, S.; George, C. Spontaneous dark formation of OH radicals at the interface of aqueous atmospheric droplets. *Proc. Natl. Acad. Sci. U.S.A.* **2023**, *120* (15), No. e2220228120.

(12) Martins-Costa, M. T. C.; Ruiz-López, M. F. Electrostatics and chemical reactivity at the air−water interface. *J. Am. Chem. Soc.* **2023**, *145* (2), 1400−1406.

(13) Jin, S.; Chen, H.; Yuan, X.; Xing, D.; Wang, R.; Zhao, L.; Zhang, D.; Gong, C.; Zhu, C.; Gao, X.; Chen, Y.; Zhang, X. The spontaneous electron-mediated redox processes on sprayed water microdroplets. *JACS Au* **2023**, *3* (6), 1563−1571.

(14) Quigley, T. M.; Mackenzie, A. S. The temperatures of oil and gas formation in the sub-surface. *Nature* **1988**, *333* (6173), 549−552.

(15) Stolper, D. A.; Lawson, M.; Davis, C. L.; Ferreira, A. A.; Neto, E. V. S.; Ellis, G. S.; Lewan, M. D.; Martini, A. M.; Tang, Y.; Schoell, M.; Sessions, A. L.; Eiler, J. M. Formation temperatures of thermogenic and biogenic methane. *Science* **2014**, *344* (6191), 1500−1503.

(16) Zengler, K.; Richnow, H. H.; Rosselló-Mora, R.; Michaelis, W.; Widdel, F. Methane formation from long-chain alkanes by anaerobic microorganisms. *Nature* **1999**, *401* (6750), 266−269.

(17) Lebel, E. D.; Lu, H. S.; Vielstädte, L.; Kang, M.; Banner, P.; Fischer, M. L.; Jackson, R. B. Methane emissions from abandoned oil and gas wells in California. *Environ. Sci. Technol.* **2020**, *54* (22), 14617−14626.

(18) Kang, M.; Christian, S.; Celia, M. A.; Mauzerall, D. L.; Bill, M.; Miller, A. R.; Chen, Y.; Conrad, M. E.; Darrah, T. H.; Jackson, R. B. Identification and characterization of high methane-emitting abandoned oil and gas wells. *Proc. Natl. Acad. Sci. U. S. A.* **2016**, *113* (48), 13636−13641.

(19) Saint-Vincent, P. M. B.; Reeder, M. D.; Sams, J. I.; Pekney, N. J. An analysis of abandoned oil well characteristics affecting methane emissions estimates in the Cherokee Platform in eastern Oklahoma. *Geophys. Res. Lett.* **2020**, *47* (23), No. e2020GL089663.

(20) Baker, C. Calculated volume and pressure changes during the thermal cracking of oil to gas in reservoirs. *AAPG Bull.* **1990**, *74* (8), 1254−1261.

(21) Umar, A. A.; Saaid, I. B. M.; Sulaimon, A. A.; Pilus, R. B. M. A review of petroleum emulsions and recent progress on water-in-crude oil emulsions stabilized by natural surfactants and solids. *J. Pet. Sci. Eng.* **2018**, *165*, 673−690.

(22) El-Adawy, M.; Ismael, M. A.; Dalha, I. B.; Aziz, A. R. A.; El Maghlany, W. Unveiling the status of emulsified water-in-diesel and nanoparticles on diesel engine attributes. *Case Stud. Therm. Eng* **2023**, *44*, No. 102824, DOI: 10.1016/j.csite.2023.102824.

(23) De Giorgi, M. G.; Fontanarosa, D.; Ficarella, A.; Pescini, E. Effects on performance, combustion and pollutants of water emulsified fuel in an aeroengine combustor. *Appl. Energy* **2020**, *260*, No. 114263.

(24) Rostampour, A.; Shojaeefard, M. H.; Molaeimanesh, G. R. Role of water micro-explosion on fuel droplet size distribution, engine performance, and emissions in a water-diesel emulsified engine: A comprehensive numerical investigation. *Int. J. Engine Res.* **2023**, *24* (3), 1110−1120.

(25) Jin, C.; Wei, J. The combined effect of water and nanoparticles on diesel engine powered by biodiesel and its blends with diesel: A review. *Fuel* **2023**, *343*, No. 127940.

(26) Merouani, S.; Hamdaoui, O.; Rezgui, Y.; Guemini, M. Sensitivity of free radicals production in acoustically driven bubble to the ultrasonic frequency and nature of dissolved gases. *Ultrasonics Sonochem.* **2015**, *22*, 41−50.

(27) Riesz, P.; Berdahl, D.; Christman, C. L. Free radical generation by ultrasound in aqueous and nonaqueous solutions. *Environ. Health Perspect.* **1985**, *64*, 233−252.

(28) Riesz, P.; Kondo, T. Free radical formation induced by ultrasound and its biological implications. *Free Radical Biol. Med.* **1992**, *13* (3), 247−270.
(29) Seo, T.; Kurokawa, R.; Sato, B. A convenient method for determining the concentration of hydrogen in water: use of methylene blue with colloidal platinum. *Med. Gas Res.* **2012**, *2* (1), 1.
(30) Pullanchery, S.; Kulik, S.; Rehl, B.; Hassanali, A.; Roke, S. Charge transfer across C−H···O hydrogen bonds stabilizes oil droplets in water. *Science* **2021**, *374* (6573), 1366−1370.
(31) Lacks, D. J.; Shinbrot, T. Long-standing and unresolved issues in triboelectric charging. *Nat. Rev. Chem.* **2019**, *3* (8), 465−476.
(32) Lin, S.; Cao, L. N. Y.; Tang, Z.; Wang, Z. L. Size-dependent charge transfer between water microdroplets. *Proc. Natl. Acad. Sci. U.S.A.* **2023**, *120* (31), No. e2307977120.
(33) Berbille, A.; Li, X.; Su, Y.; Li, S.; Zhao, X.; Zhu, L.; Wang, Z. L. Mechanism for generating H_2O_2 at water-solid interface by contact-electrification. *Adv. Mater.* **2023**, 2304387.
(34) Xia, Y.; Li, J.; Zhang, Y.; Yin, Y.; Chen, B.; Liang, Y.; Jiang, G.; Zare, R. N. Contact between water vapor and silicate surface causes abiotic formation of reactive oxygen species in an anoxic atmosphere. *Proc. Natl. Acad. Sci. U.S.A.* **2023**, *120* (30), No. e2302014120.
(35) Gong, C.; Li, D.; Li, X.; Zhang, D.; Xing, D.; Zhao, L.; Yuan, X.; Zhang, X. Spontaneous reduction-induced degradation of viologen compounds in water microdroplets and its inhibition by host−guest complexation. *J. Am. Chem. Soc.* **2022**, *144* (8), 3510−3516.
(36) Chen, H.; Wang, R.; Xu, J.; Yuan, X.; Zhang, D.; Zhu, Z.; Marshall, M.; Bowen, K.; Zhang, X. Spontaneous reduction by one electron on water microdroplets facilitates direct carboxylation with CO_2. *J. Am. Chem. Soc.* **2023**, *145* (4), 2647−2652.
(37) Yuan, X.; Zhang, D.; Liang, C.; Zhang, X. Spontaneous reduction of transition metal ions by one electron in water microdroplets and the atmospheric implications. *J. Am. Chem. Soc.* **2023**, *145* (5), 2800−2805.
(38) Qiu, L.; Cooks, R. G. Simultaneous and spontaneous oxidation and reduction in microdroplets by the water radical cation/anion pair. *Angew. Chem., Int. Ed.* **2022**, *61* (41), No. e202210765.
(39) Colussi, A. J. Mechanism of hydrogen peroxide formation on sprayed water microdroplets. *J. Am. Chem. Soc.* **2023**, *145* (30), 16315−16317.
(40) Zhang, D.; Yuan, X.; Gong, C.; Zhang, X. High electric field on water microdroplets catalyzes spontaneous and ultrafast oxidative C-H/N-H cross-coupling. *J. Am. Chem. Soc.* **2022**, *144* (35), 16184−16190.
(41) Santos, L. P.; Lermen, D.; Yoshimura, R. G.; da Silva, B. L.; Galembeck, A.; Burgo, T. A. L.; Galembeck, F. Water reactivity in electrified interfaces: The simultaneous production of electricity, hydrogen, and hydrogen peroxide at room temperature. *Langmuir* **2023**, *39* (16), 5840−5850.
(42) Zhou, Z.; Zhang, C. j.; Liu, P. f.; Fu, L.; Laso-Pérez, R.; Yang, L.; Bai, L. p.; Li, J.; Yang, M.; Lin, J. z.; Wang, W. d.; Wegener, G.; Li, M.; Cheng, L. Non-syntrophic methanogenic hydrocarbon degradation by an archaeal species. *Nature* **2022**, *601* (7892), 257−262.
(43) Zhang, Y.-J.; Chen, J.-J.; Huang, G.-X.; Li, W.-W.; Yu, H.-Q.; Elimelech, M. Distinguishing homogeneous advanced oxidation processes in bulk water from heterogeneous surface reactions in organic oxidation. *Proc. Natl. Acad. Sci. U. S. A.* **2023**, *120* (20), No. e2302407120, DOI: 10.1073/pnas.2302407120.
(44) Enami, S.; Sakamoto, Y.; Colussi, A. J. Fenton chemistry at aqueous interfaces. *Proc. Natl. Acad. Sci. U. S. A.* **2014**, *111* (2), 623−628.
(45) Müller, I. B.; Cederbaum, L. S. Ionization and double ionization of small water clusters. *J. Chem. Phys.* **2006**, *125* (20), 204305 DOI: 10.1063/1.2357921.
(46) Zhou, Z.; Zhang, L.; Xie, M.; Wang, Z.; Chen, D.; Qi, F. Determination of absolute photoionization cross-sections of alkanes and cyclo-alkanes. *Rapid Commun. Mass Spectrom.* **2010**, *24* (9), 1335−1342.
(47) Bellville, D. J.; Bauld, N. L. Elongated (one-electron) carbon-carbon bond in σ and n organic cation radicals. *J. Am. Chem. Soc.* **1982**, *104* (21), 5700−5702.
(48) Fokin, A. A.; Schreiner, P. R. Selective alkane transformations via radicals and radical cations: Insights into the activation step from experiment and theory. *Chem. Rev.* **2002**, *102* (5), 1551−1594.
(49) Kim, S. H.; Betty, K. R.; Karasek, F. W. Mobility behavior and composition of hydrated positive reactant ions in plasma chromatography with nitrogen carrier gas. *Anal. Chem.* **1978**, *50* (14), 2006−2012.
(50) Cai, J.; Griffin, E.; Guarochico-Moreira, V. H.; Barry, D.; Xin, B.; Yagmurcukardes, M.; Zhang, S.; Geim, A. K.; Peeters, F. M.; Lozada-Hidalgo, M. Wien effect in interfacial water dissociation through proton-permeable graphene electrodes. *Nat. Commun.* **2022**, *13* (1), 5776.
(51) Lee, J. K.; Walker, K. L.; Han, H. S.; Kang, J.; Prinz, F. B.; Waymouth, R. M.; Nam, H. G.; Zare, R. N. Spontaneous generation of hydrogen peroxide from aqueous microdroplets. *Proc. Natl. Acad. Sci. U. S. A.* **2019**, *116* (39), 19294−19298.
(52) Ben-Amotz, D. Electric buzz in a glass of pure water. *Science* **2022**, *376* (6595), 800−801.
(53) Song, X.; Basheer, C.; Zare, R. N. Making ammonia from nitrogen and water microdroplets. *Proc. Natl. Acad. Sci. U.S.A.* **2023**, *120* (16), No. e2301206120.
(54) Buxton, G. V.; Greenstock, C. L.; Helman, W. P.; Ross, A. B. Critical review of rate constants for reactions of hydrated electrons, hydrogen atoms and hydroxyl radicals (·OH/·O^- in aqueous solution. *J. Phys. Chem. Ref. Data* **1988**, *17* (2), 513−886.
(55) Poli, E.; Jong, K. H.; Hassanali, A. Charge transfer as a ubiquitous mechanism in determining the negative charge at hydrophobic interfaces. *Nat. Commun.* **2020**, *11* (1), 901.
(56) Pezzotti, S.; Serva, A.; Gaigeot, M. P. 2D-HB-Network at the air-water interface: A structural and dynamical characterization by means of ab initio and classical molecular dynamics simulations. *J. Chem. Phys.* **2018**, *148* (17), 174701.
(57) Kallbekken, S.; Victor, D. G. A cleaner future for flight—aviation needs a radical redesign. *Nature* **2022**, *609* (7928), 673−675.
(58) Lee, D. S.; Fahey, D. W.; Skowron, A.; Allen, M. R.; Burkhardt, U.; Chen, Q.; Doherty, S. J.; Freeman, S.; Forster, P. M.; Fuglestvedt, J.; Gettelman, A.; De León, R. R.; Lim, L. L.; Lund, M. T.; Millar, R. J.; Owen, B.; Penner, J. E.; Pitari, G.; Prather, M. J.; Sausen, R.; Wilcox, L. J. The contribution of global aviation to anthropogenic climate forcing for 2000 to 2018. *Atmos. Environ.* **2021**, *244*, No. 117834.
(59) Sofiev, M.; Winebrake, J. J.; Johansson, L.; Carr, E. W.; Prank, M.; Soares, J.; Vira, J.; Kouznetsov, R.; Jalkanen, J. P.; Corbett, J. J. Cleaner fuels for ships provide public health benefits with climate tradeoffs. *Nat. Commun.* **2018**, *9* (1), 406.
(60) Sartomo, A.; Santoso, B.; Ubaidillah; Muraza, O. Recent progress on mixing technology for water-emulsion fuel: A review. *Energy Convers. Manage.* **2020**, *213*, No. 112817.